Liquid Crystals
Publication details, including instructions for authors and subscription information:
http://www.informaworld.com/smpp/title~content=t713926090

The hexagonal to discotic phase transition in 1,4,8,11,15,18,22,25-octahexylphthalocyanine studied by differential scanning calorimetry

Ahmad A. Joraid[a]; Saleh N. Alamri[a]; Shaya Y. Al-Raqa[b]; Ahmed A. Mohamed[b]
[a] Department of Physics, Taibah University, Madinah, Saudi Arabia [b] Department of Chemistry, Taibah University, Madinah, Saudi Arabia

To cite this Article Joraid, Ahmad A. , Alamri, Saleh N. , Al-Raqa, Shaya Y. and Mohamed, Ahmed A.(2008) 'The hexagonal to discotic phase transition in 1,4,8,11,15,18,22,25-octahexylphthalocyanine studied by differential scanning calorimetry', Liquid Crystals, 35: 3, 351 — 356
To link to this Article: DOI: 10.1080/02678290701847885
URL: http://dx.doi.org/10.1080/02678290701847885

Liquid Crystals,
Vol. 35, No. 3, March 2008, 351–356

Taylor & Francis
Taylor & Francis Group

The hexagonal to discotic phase transition in 1,4,8,11,15,18,22,25-octahexylphthalocyanine studied by differential scanning calorimetry

Ahmad A. Joraid[a]*, Saleh N. Alamri[a], Shaya Y. Al-Raqa[b] and Ahmed A. Mohamed[b]*

[a]*Department of Physics, Taibah University, Madinah, Saudi Arabia;* [b]*Department of Chemistry, Taibah University, Madinah, Saudi Arabia*

(Received 8 October 2007; final form 6 December 2007)

The phase change in metal-free 1,4,8,11,15,18,22,25-octahexylphthalocyanine compound with eight non-peripheral hexyl chains was investigated under non-isothermal conditions by differential scanning calorimetry (DSC) and scanning electron microscopy (SEM). Two endothermic changes were reported. The first one between 332 and 350 K relates to the transition from the hexagonal columnar mesophase to a less ordered crystalline phase, P_1. The second endothermic transition from 408 to 417 K is due to the transition to the discotic columnar mesophase, P_2. The isoconversional methods of Friedman, and Kissinger, Akahira and Sunose (KAS) were used to determine the variation of the activation energy for crystallisation with temperature, $E_\alpha(T)$. Using the Friedman method the average values of $E_\alpha(T)$ were 121.31 and 352.77 kJ mol^{-1} for the first and second peaks, respectively. The KAS method gave higher values of $E_\alpha(T)$ with averages of 173.25 and 411.44 kJ mol^{-1}, respectively. The specific heat was measured and found to vary with temperature.

Keywords: Phthalocyanine; Phase Transition; Discotic; Hexagonal; Activation Energy; Specific Heat

1. Introduction

Phthalocyanines have many important commercial applications as colourants for fabrics, printing inks, ball points and colour photography. They are best known for their intense blue or blue-green colours, their thermal and chemical stability, and their ability to incorporate, into the centre of their ring system, about 70 elements of the periodic table. Their properties depend on their X-ray structures and in particular on their crystal packing arrangements. Phthalocyanines represent one of the most extensively studied classes of compounds (*1–3*).

Liquid crystalline phthalocyanines offer the possibility of combining their optoelectronic properties with the orientation control of conventional liquid crystal systems. The columnar architecture of the substituted phthalocyanines suggests the possibility of using them as anisotropic conductors. Discotic columnar liquid crystals have drawn much attention as semiconductors, molecular wires, photovoltaic cells and light emitting diodes (*4*). Many soluble phthalocyanines such as $(C_nS)_8PcCu$, n=8, 10, 12, 16, exhibit a columnar mesophase (*5*) and heating above the mesophase transition can improve their columnar ordering (*6*). This alkylthio phthalocyanine forms a columnar hexagonal mesophase over a wide temperature range.

Several liquid crystalline phthalocyanine compounds with numerous substituents have been synthesised to produce more easily controllable macroscopic structures. Although many liquid crystalline phthalocyanine compounds having peripheral alkyloxy and alkylthio chains have been prepared, little work has been done on the peripheral alkyl chains and the effect of temperature on the activation energy and specific heat of mesomorphic behaviour of these compounds (*7*). By functionalising the phthalocyanine ring with long aliphatic chains the solubility increases and liquid crystalline compounds can be obtained. Cook (*8*) synthesised cobalt (II) phthalocyanines with eight non-peripheral alkyl chains, which show a hexagonal columnar mesophase between 75 and 189°C.

Our work with phthalocyanine chemistry first resulted in the synthesis and characterisation of symmetrical hexadeca-substituted phthalocyanato zinc (II) compounds. Thin films of the prepared Zn phthalocyanines were deposited by using spin coating techniques onto microscope slide substrates, and their structural and optical parameters were described (*9*). We describe the hexagonal to discotic phase transition and the effect of temperature on the activation energy and specific heat on the transition in metal-free 1,4,8,11,15,18,22,25-octahexylphthalocyanine compound, H_2Pc.

2. Experimental

Synthesis

The metal-free phthalocyanine compound used in this study was prepared directly by cyclotetramerisation of 3,6-dihexylphthalonitrile in the presence of

*Corresponding authors. Email: aaljoraid@taibahu.edu.sa; amohamed@mail.chem.tamu.edu

ISSN 0267-8292 print/ISSN 1366-5855 online

DOI: 10.1080/02678290701847885
http://www.informaworld.com

lithium butoxide in butanol. The purification steps required column chromatography on silica gel using petroleum ether as an eluent to yield 77% of 1,4,8,11,15,18,22,25-octahexylphthalocyanine compound, see Figure 1 (*9*). The Pc compound was characterised by ^{1}H nuclear magnetic resonance (NMR), mass spectrometry, and UV-Vis and IR spectroscopy. The synthesised Pc complex possesses excellent solubility in various organic solvents such as CH_2Cl_2, tetrahydrofuran (THF), acetone and ethyl acetate, and does not readily aggregate in solution.

Instrumentation

Differential scanning calorimetry (DSC) experiments were performed using a Shimadzu DSC-60 instrument, available at Taibah University, with an accuracy of ± 0.1 K under dry nitrogen supplied at a rate of 35 ml min^{-1}. The samples, of 2–3 mg, were encapsulated in standard aluminium pans.

Non-isothermal DSC curves were obtained at heating rates of β=2, 5, 10, 15, 20, 30, 40 and 50 K min^{-1}. To calculate the specific heat capacity, C_p, from the DSC measurements the Shimadzu DSC-60 workstation was equipped with a specific heat capacity program. The C_p was calculated using the following expression (*10, 11*):

$$C_{Ps} = \frac{S_s m_r}{S_r m_s} C_{Pr} \quad (1)$$

where C_{ps} and C_{pr} are the specific heat capacity of the sample and reference material, respectively.

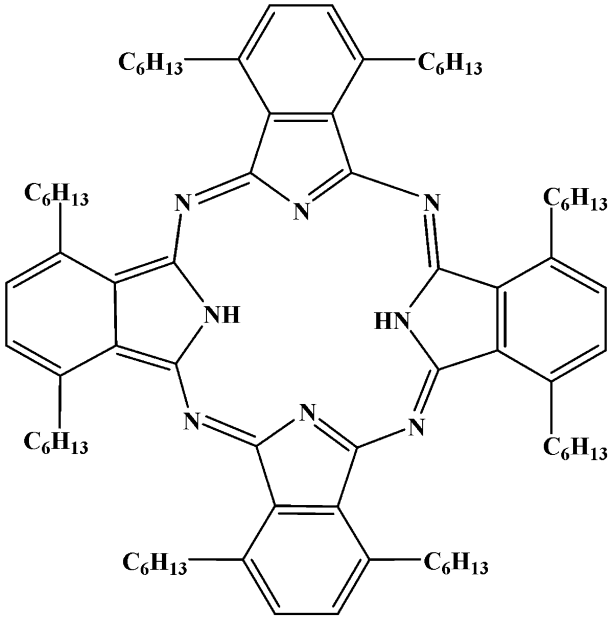

Figure 1. Structure of H_2Pc.

Parameters S_s and S_r represent the differences in heat flow between the DSC curves of the baseline and sample runs, while m_s and m_r are the masses of the sample and reference material, respectively.

Three types of specific heat capacity measurements were carried out: (i) baseline measurement; (ii) reference measurement; and (iii) sample measurement. In the baseline measurement, the empty crucible was placed in both the sample and reference holders. For the reference measurement an empty crucible was placed on the reference side holder, while another crucible with a reference material, alumina, was placed on the sample side holder. In the sample measurement, an empty crucible and a crucible with the sample were loaded at the reference and sample side holders. A three-step heating program was applied for the measurements: (i) isothermal heating at 313 K for 3 min; (ii) dynamic heating from 313 to 423 K at a heating rate of 5 K min^{-1}; and (iii) isothermal heating at 423 K for 3 min. The temperature and enthalpy calibrations were checked against an indium standard sample (T_m=156.6°C and ΔH_m=28.55 J g^{-1}) supplied by Shimadzu.

3. Results and discussion

Phase transition

DSC measurements were conducted on a sample of H_2Pc by heating from 300 to 430 K (see Figure 2), at heating rates of 5, 15 and 30 K min^{-1}. Two endothermic changes were reported. The first one was between 332 and 350 K for a heating rate of 2 to 50 K min^{-1}. This initial stage relates to the transition from the hexagonal columnar mesophase to a less ordered crystalline phase, P_1 (*3*). The second endothermic transition was reported from 408 to

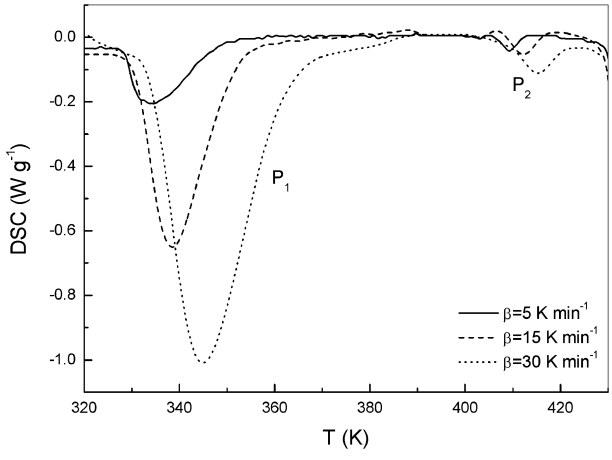

Figure 2. DSC traces at heating rates of 5, 15 and 30 K min^{-1}.

417 K for the same heating rate of 2 to 50 K min^{-1}. This change may be due to the transition to the discotic columnar mesophase, P_2, see Figure 3 (*3*). Disk-shaped mesogens can orient themselves in a layer-like fashion known as the discotic nematic phase. If the disks pack into stacks, the phase is called a discotic columnar phase. The transition from the crystal phase to the discotic columnar mesophase occurs in a number of transitions marking the stepwise reduction of the order of the sample. It is proposed that the molecules adjust towards the liquid crystal (discotic columnar) packing arrangement when the hexyl groups become completely mobile (*3*).

The change in morphology under isothermal annealing was recorded by scanning electron microscopy (SEM). The morphology of H_2Pc recovered after crystallisation at room temperature is shown in Figure 4. The micrograph shows that the crystals have a flat arrangement in tilted stacks. Figures 4(b)–(d) show the effect of heat treatment on the texture of H_2Pc under nitrogen flow. Figure 4(b) shows an SEM micrograph of the H_2Pc sample after annealing for 10 min at 334 K. The micrograph indicates that the crystallisation order is still unchanged but with some distortion. This distortion dramatically increases as the temperature increases, accompanied by formation of fine clusters of disk-like texture.

The kinetic equation combined with the Arrhenius approach to the temperature function of the reaction rate constant can be described by (*12, 13*)

$$\frac{\mathrm{d}\alpha}{\mathrm{d}t} = A\exp\left(-\frac{E}{RT}\right)f(\alpha) \qquad (2)$$

where t is the time, T is the temperature, α is the degree of conversion, A (s^{-1}) is the frequency factor, E (kJ mol^{-1}) is the effective activation energy of the phase transition, R (kJ/mol·K) is the universal gas constant and $f(\alpha)$ is the reaction model.

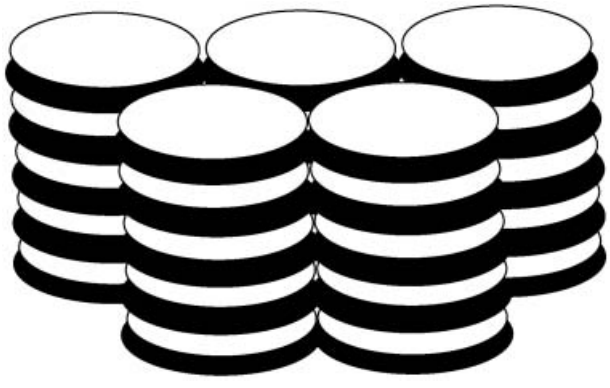

Figure 3. Representation of the discotic columnar phase.

Under non-isothermal conditions with a constant heating rate of $\beta = \mathrm{d}T/\mathrm{d}t$, equation (2) may be rewritten as

$$\frac{\mathrm{d}\alpha}{\mathrm{d}T} = \frac{\mathrm{d}\alpha}{\mathrm{d}t}\left(\frac{1}{\beta}\right) = \frac{A}{\beta}\exp\left(-\frac{E}{RT}\right)f(\alpha). \qquad (3)$$

For various heating rates, β_i, the Friedman method (*14*) can be obtained directly at a specific degree of conversion, α, as

$$\ln\left(\frac{\mathrm{d}\alpha}{\mathrm{d}t}\right)_{\alpha i} = C_{\mathrm{F}}(\alpha) - \frac{E_\alpha}{RT_{\alpha i}} \qquad (4)$$

where the subscript i denotes different heating rates and the parameter $C_{\mathrm{F}}(\alpha)$ equals $\ln(A_\alpha f(\alpha))$.

For a specific α value and several heating rates, pairs of $(\mathrm{d}\alpha/\mathrm{d}t)_{\alpha i}$ and $T_{\alpha i}$ are determined experimentally from the DSC thermograph. The parameters E_α and $C_F(\alpha)$, at this specific value of α, are then estimated from the plot of $\ln(\mathrm{d}\alpha/\mathrm{d}t)_{\alpha i}$ versus $1/T_{\alpha i}$ (equation (4)) across at least three different heating rates. The procedure is repeated for several α values to yield continuous functions of α for E_α and $C_{\mathrm{F}}(\alpha)$. The dependence of E_α on temperature can be obtained by replacing α with the respective temperature interval (*13*).

Results using the Kissinger–Akahira–Sunose (KAS) method (*15–17*) may be obtained from the derivation of equation (3). Subsequent application of the logarithm and rearrangement yields

$$\ln\left(\frac{\beta_i}{T_{\alpha i}^2}\right) = C_{\mathrm{K}}(\alpha) - \frac{E_\alpha}{RT_{\alpha i}} \qquad (5)$$

where

$$C_{\mathrm{K}}(\alpha) = \ln\left[\left|\frac{\mathrm{d}f(\alpha)}{\mathrm{d}\alpha}\right|\frac{AR}{E_\alpha}\right].$$

The experimental determination of E_α and $C_{\mathrm{K}}(\alpha)$ is similar to that used by the Friedman method. For each degree of the conversion fraction, α, a corresponding $T_{\alpha i}$ and heating rate are used to plot $\ln(\beta_i/T^2{}_{\alpha i})$ against $1/T_{\alpha i}$. The parameters E_α and $C_{\mathrm{K}}(\alpha)$ are then determined from the regression slope and intercept.

However, in a typical experiment it is necessary to obtain at least three different heating rates (β_i) and the respective conversion curves are evaluated from the measured DSC curves. For each conversion (α), either $\ln(\mathrm{d}\alpha/\mathrm{d}t)_{\alpha i}$ is plotted against $1/T_{\alpha i}$, which is the basis of the Friedman method, or $\ln(\beta_i/T^2{}_{\alpha i})$ is plotted against $1/T_{\alpha i}$, which is the basis of the KAS method.

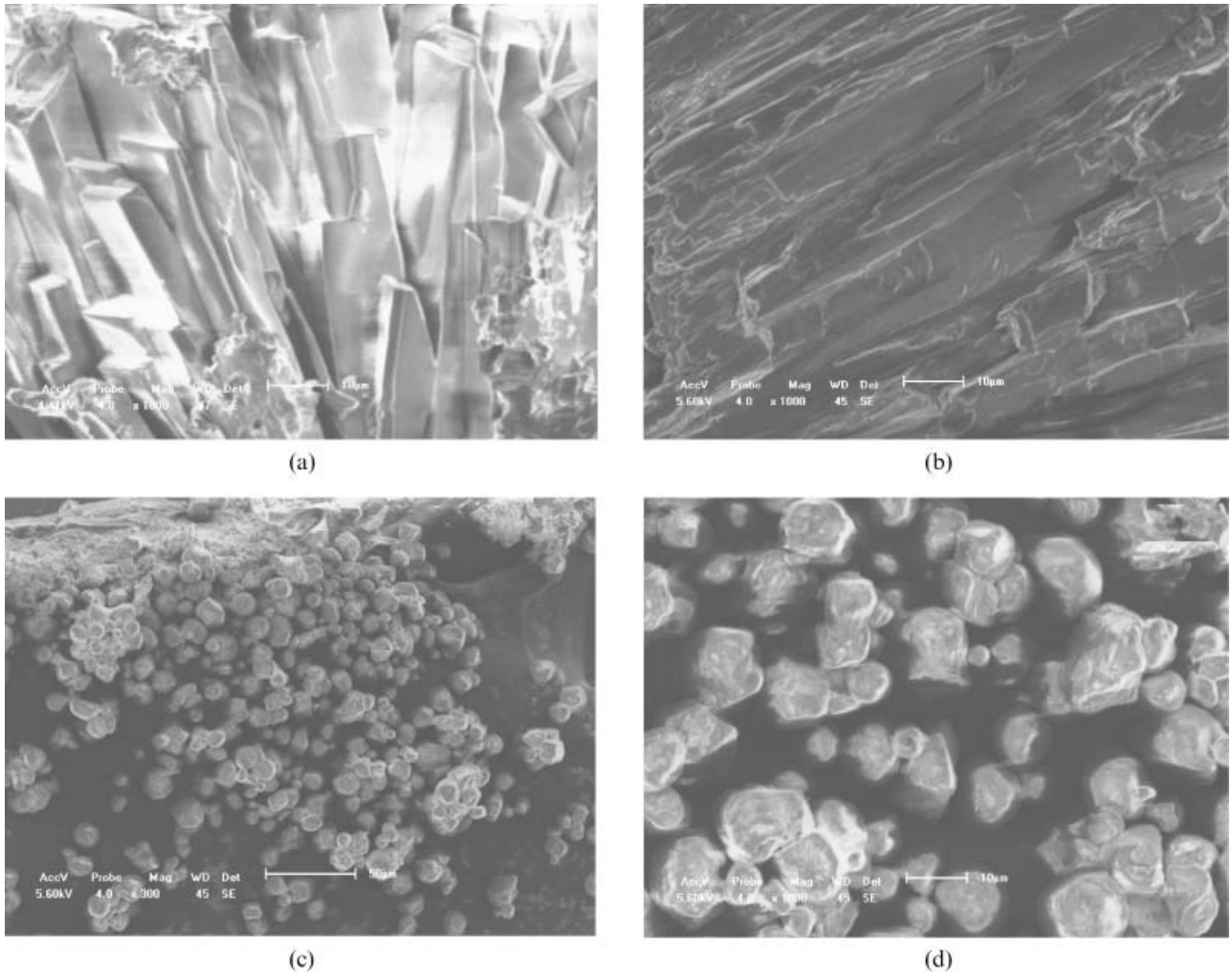

Figure 4. (a) The electron microscopy pattern of H_2Pc as-prepared; electron microscopy patterns of H_2Pc annealed for 10 min under nitrogen flow at (b) 334 K, (c) 409 K ($\times 300$), and (d) 409 K ($\times 1000$).

This will give a straight line with slope $-E_\alpha/R$, and therefore the activation energy is obtained as a function of conversion.

The variation curves of the conversion rate, α, with temperature at different heating rates, β_i, for the two phases P_1 and P_2 are shown in Figure 5. Increasing the heating rate leads to an increase in the peak temperature. The E_α values calculated by the KAS method are higher than those calculated by the Friedman method (*13, 18–20*). The differences are due to the approximation of the temperature integral used in the derivations of the relations that ground the KAS and non-linear methods (*18*). The significant differences between the apparent activation energy calculated by the Friedman method (with average values of E_α=121.31 and 352.77 kJ mol^{-1} for P_1 and P_2, respectively) and the values of E_α calculated using the KAS method (with average values of E_α=173.25 and 411.44 kJ mol^{-1} for P_1 and P_2, respectively) are due

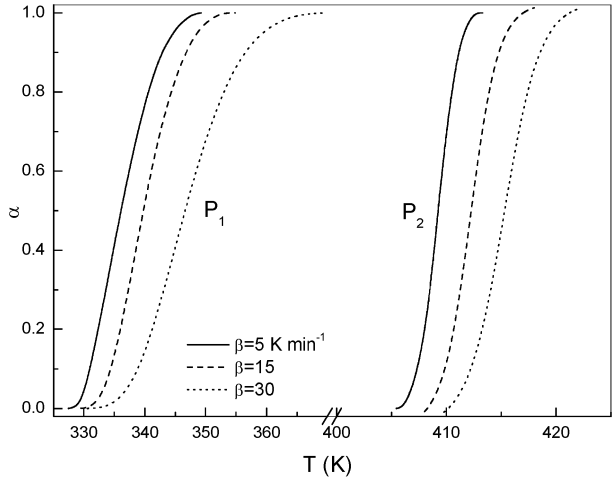

Figure 5. Degree of conversion, α, as a function of temperature at different heating rates for the two phases P_1 and P_2.

to the way by which the mathematical relations that form the basis of the 'integral' methods are derived.

Figure 6 shows the variation of the activation energy, E_α, as a function of the extent of conversion, α, for H_2Pc obtained at the heating rate, β, in the range 2–50 K min^{-1}. For the first transition, P_1, Figure 6, the same shapes are obtained for the curves of E_α versus α using both isoconversional methods. The two curves show that E_α decreases with the extent of conversion, α, noting that two different regions exist. E_α rapidly decreases in the conversion range $0.05 \leqslant \alpha \leqslant 0.3$, and after this range ($\alpha > 0.3$), a decrease of E_α with α continues approximately linearly.

The observed E_α versus α values for the second peak transition, P_2, show different behaviour at the initial stage in the Friedman and KAS methods. The Friedman method shows that E_α rapidly decreases in the conversion range $0.05 \leqslant \alpha \leqslant 0.3$. After the range $0.03 \leqslant \alpha \leqslant 0.8$, E_α decreases approximately linearly with α followed by a strong decrease of E_α after $\alpha > 0.8$. The KAS method shows that the activation energy is initially low and increases in the conversion range $0.05 \leqslant \alpha \leqslant 0.15$. The conversion rate then gradually decreases in the limits $0.15 \leqslant \alpha \leqslant 0.8$, and strongly decreases again at $\alpha > 0.8$.

The $E_\alpha(T)$ dependence curves for the two phases, Figure 7, reveal typical endothermic reversible reactions (*20*). The E_α values are positive and decrease with temperature for the two methods used, which simply indicates that the phase transition rate increases as the temperature increases. This behaviour demonstrates that the rate of the phase transition is in fact determined by more than one mechanism (*12, 20–22*).

Specific heat capacity

In line with the procedure described in the experimental section, a typical DSC thermogram output for

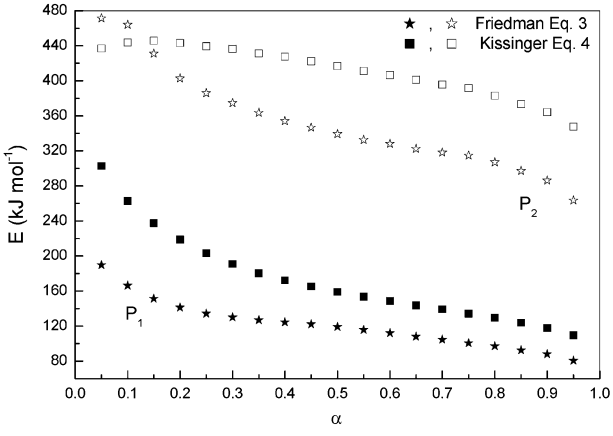

Figure 6. Dependence of the activation energy of the phase transition, E_α, on the degree of conversion, α.

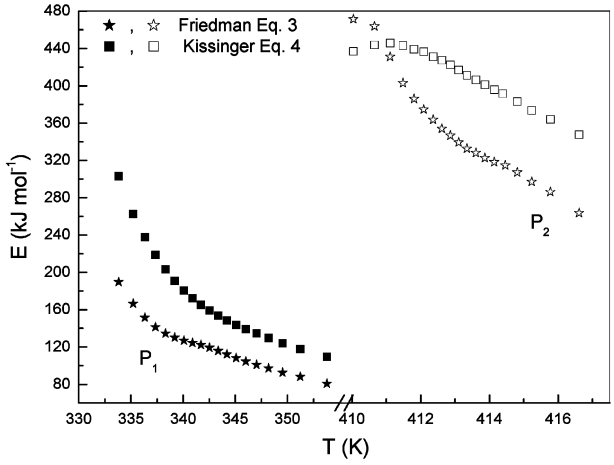

Figure 7. Dependence of the activation energy, E_α, of the phase transition on temperature.

C_p determination is given in Figure 8. Curve A represents the baseline while curves B and C represent the DSC traces of the reference and sample, respectively. Curve D shows the heating progress. The difference between the baseline and sample DSC curves represents the heat consumed by the sample during the heating progress. The sample could be tested up to a temperature of about 420 K. The samples begin to melt at higher temperatures. The calculated results of the specific heat capacity of H_2Pc, Figure 9, show that the specific heat capacity increases with increasing temperature. The two peaks at about 333.8 and 409.7 K are due to the phase changes P_1 and P_2, respectively. If these two peaks are extracted, the specific heat capacity can be fitted to a second-order polynomial ($C_p = 1.9 - 0.01T + 1.9 \times 10^{-5} T^2$) with a correlation coefficient of 0.991, (Figure 9). The correlation coefficient reflects the degree of the

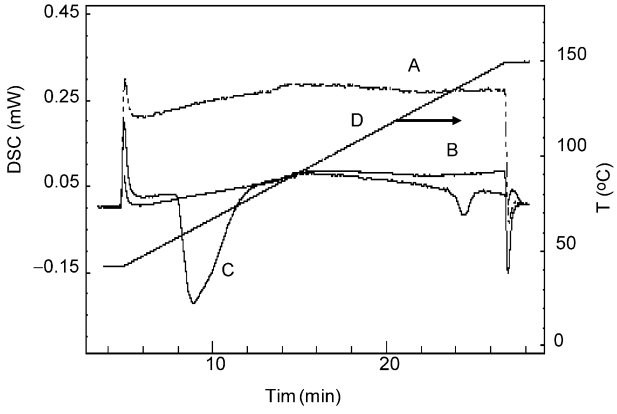

Figure 8. A typical thermogram of the specific heat capacity determination for H_2Pc by DSC. Curve A shows the baseline while curves B and C represent the DSC traces of the reference and sample, respectively. Curve D shows the heating progress.

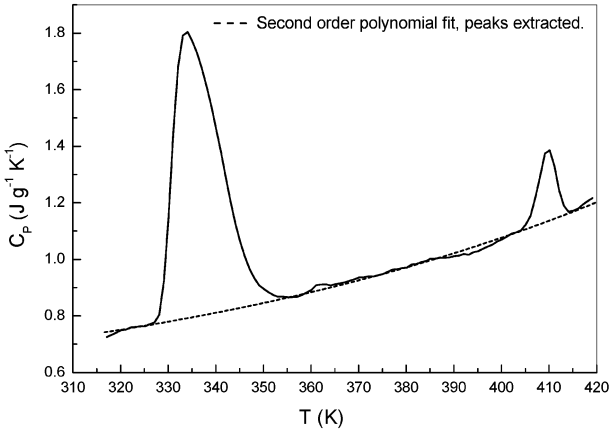

Figure 9. The specific heat capacity for H_2Pc versus temperature.

linear relationship between the two variables specific heat capacity and temperature. The linear regression equation (C_p=0.044T−0.071) can be obtained in the temperature range 354–405 K with a correlation coefficient of 0.987. This shows that the variation of the specific heat capacity with temperature has a great influence on the phase transition.

4. Conclusions

We have described the phase transition in metal-free 1,4,8,11,15,18,22,25-octahexylphthalocyanine at different heating rates under nitrogen atmosphere by the use of DSC. Two endothermic changes were described and investigated. First, by applying two isoconversion methods (Friedman and KAS), the activation energies of crystallisation, $E_\alpha(T)$, show a strong decrease with increasing temperature for both peaks. The values of the activation energy calculated by the Friedman method gave average values of E_α=121.31 and 352.77 kJ mol^{-1} for the first and second peaks, respectively, whilst the calculated values of E_α using the KAS method gave average values of 173.25 and 411.44 kJ mol^{-1}, respectively.

The specific heat of metal-free 1,4,8,11,15,18,22,25-octahexylphthalocyanine was measured by a DSC technique. Two peaks were recognised at 333.8 and 409.7 K. By extracting these two peaks the specific heat followed a second-order polynomial relationship with temperature.

We are continuing our study on the hexagonal to discotic phase transition and the activation energy for conduction in perfluorinated phthalocyanines. In particular, we are interested in the effect of the π–π overlap in the perfluorinated phthalocyanines in a columnar stack. The phase transition in metal containing phthalocyanines will be studied versus that for metal-free derivatives.

Acknowledgement

The authors are grateful for the support of Taibah University Faculty Grant (23/427).

References

(1) Leznoff C.C.; Lever A.B.P. *Phthalocyanine-Properties and Applications*; Vol. 1; VCH: New York, 1989.
(2) Leznoff C.C.; Lever A.B.P. *Phthalocyanine-Properties and Applications*; Vol. 3; VCH: New York, 1993.
(3) Helliwell M.; Teat S.J.; Coles S.J.; Reeve W. *Acta Cryst.* **2003**, *B59*, 617–624.
(4) Simon J.; Bassoul P. *Design of Molecular Materials; Supramolecular Engineering*; Wiley: New York, 2000.
(5) Ban K.; Nishizawa K.; Ohta K.; Shirai H. *J. Mater. Chem.* **2000**, *10*, 1083–1090.
(6) (a) Cook M.J.; Mayes D.A.; Poynter R.H. *J. Mater. Chem.* **1995**, *5*, 2233–2238, (b) T. Basanova, A.G. Gurek, V. Ahsen. *Mater. Sci. Eng.*, **2002**, *C22*, 99–104.
(7) (a) Engel M.K.; Bassoul P.; Bosio L.; Lehmann H.; Hanack M.; Simon J. *Liq. Cryst.* **1993**, *15*, 709–722, (b) Basanova T.; Gurek A.G.; Ahsen V. *Mater. Sci. Eng.* **2002**, *C22*, 99, (c) A.S. Cherodian, A.N. Davies, R.M. Richardson, M.J. Cook, N.B. McKeown, A.J. Thomson, J. Feijoo, G. Ungar and K.J. Harrison. *Molecular Crystals and Liquid Crystals*, **1991**, *196*, 103–114.
(8) Cook M.J. *J. Mater. Sci.: Mater. Electron.* **1994**, *5*, 117–128.
(9) (a) Alamri S.N.; Joraid A.A.; Al-Raqa S.Y. *Thin Solid Films* **2006**, *510*, 265–270, (b) S.Y. Al-Raqa, A.S. Solieman, A.A. Joraid, S.N. Alamri, Z. Moussa and A. Aljuhani. *Polyhedron*, **2008**, *27*, 1256–1261.
(10) Cherodian A.S.; Davis A.N.; Richardson R.M. *Molec. Crystals Liq. Crystals* **1991**, *196*, 103.
(11) Gupta M.; Yang J.; Roy C. *Fuel* **2003**, *82*, 919–927.
(12) Vyazovkin S.; Sbirrazzuoli N. *Macromol. Rapid Commun.* **2006**, *27*, 1515–1532.
(13) Joraid A.A. *Thermochim. Acta* **2007**, *456*, 1–6.
(14) Friedman H.L. *J. Polym. Sci.* **1964**, *C6*, pp. 183–195.
(15) Kissinger H.E. *J. Res. Nat. Bureau Standards* **1956**, *57*, 217–221.
(16) Kissinger H.E. *Anal. Chem.* **1957**, *29*, 1702–1706.
(17) Akahira T.; Sunose T. *Res. Report Chiba Inst. Technol.* **1971**, *16*, 22–31.
(18) Budrugeac P.; Homentcovschi D.; Segal E. *J. Therm. Anal. Cal.* **2001**, *66*, 557–565.
(19) Joraid A.A. *Physica B* **2007**, *390*, 263–269.
(20) Jankovic B.; Adnadevic B.; Jovanovic J. *Thermochim. Acta* **2007**, *452*, 106–115.
(21) Vyazovkin S.; Dranca I. *Macromol. Chem. Phys.* **2006**, *207*, 20–25.
(22) Vyazovkin S. *J. Therm. Anal. Cal.* **2006**, *83*, 45–51.
(23) Joraid A.A. *Physica B* **2007**, *390*, 263.
(24) Jankovic B.; Adnadevic B.; Jovanovic J. *Thermochim. Acta* **2007**, *452*, 106.
(25) Vyazovkin S.; Dranca I. *Macromol. Chem. Phys.* **2006**, *207*, 20.
(26) Vyazovkin S. *J. Therm. Anal. Cal.* **2006**, *83*, 45.